Quantitative geometric analysis of rib, costal cartilage and sternum from childhood to teenagehood

Baptiste Sandoz [1], Alina Badina [2], Sébastien Laporte [1], Karene Lambot [3], David Mitton [1], Wafa Skalli [1]

[1]Arts et Metiers ParisTech, LBM, 151 bd de l'Hopital 75013 Paris, France

[2] Université Paris Descartes, Faculté de Médecine, Hôpital Necker, Service d'orthopédie pédiatrique, 149 rue de Sèvre, 75015, Paris, France

[3] Université Paris Descartes, Faculté de Médecine, Hôpital Necker, Service de radiologie pédiatrique, 149 rue de Sèvre, 75015, Paris, France

Corresponding author:

Dr Baptiste Sandoz
baptiste.sandoz@ensam.eu

Arts et Metiers ParisTech, LBM, 151 boulevard de l'hopital, 75013 Paris, France

Tel: +33 1 44 24 63 64
Fax: +33 1 44 24 63 66

Total word count: 3699
Abstract word count: 193
Number of Figures: 6
Number of Tables: 1
Complementary material: 1

Abstract

Better understanding of the effects of growth on children's bones and cartilage is necessary for clinical and biomechanical purposes. The aim of this study is to define the 3D geometry of children's rib cages: including sternum, ribs and costal cartilage. Three-dimensional reconstructions of 960 ribs, 518 costal cartilages and 113 sternebrae were performed on thoracic CT-scans of 48 children, aged four months to 15 years. The geometry of the sternum was detailed and nine parameters were used to describe the ribs and rib cages. A "costal index" was defined as the ratio between cartilage length and whole rib length to evaluate the cartilage ratio for each rib level. For all children, the costal index decreased from rib level one to three and increased from level three to seven. For all levels, the cartilage accounted for 45 to 60% of the rib length, and was longer for the first years of life. The mean costal index decreased by 21% for subjects over three years old compared to those under three ($p<10^{-4}$). The volume of the sternebrae was found to be highly age dependent. Such data could be useful to define the standard geometry of the paediatric thorax and help to detect clinical abnormalities.

Keywords: *child; rib; cartilage; thorax; sternum*

1. Introduction

The thoracic anatomy of children is clinically important in spinal deformities such as scoliosis, and anatomical measurements can be used to identify normal geometry, quantify the severity of deformity, evaluate pulmonary capacity or build models for orthopedic or surgical treatment. Moreover, the thorax contains and protects vital organs and can be injured when subjected to impact, as in motor vehicle accidents. For children, the thorax is the second most often injured segment in crash events [5].

Child external morphology is well known, and some specific databases have been created to design child dummies [9, 26, 29]. However costal cartilage and sternal anatomy are generally not assessed, even though they can be of primary importance. The rib ossification process progressively increases the stiffness of the thorax and sets final thoracic geometry. During ribcage ossification, the large difference in material properties between cartilage and bone affects the stiffness of the rib cage, which is important when considering the orthotic brace effect or response to an impact in children.

Child thorax geometry is often described to highlight specific abnormalities (scoliosis, pectus carinatum and pectus excavatum), but quantitative descriptions of child ribcages are rare, while they are essential to build numerical models or to identify normal patterns for different age groups. Only a few existing studies provide descriptive parameters of the child rib cage. Derveaux et al. used 2D measurements on lateral X-rays to evaluate the anteroposterior width of the thorax [11]. On CT-Scan slices, Haller et al. defined an index to describe the ratio between the transversal and anteroposterior diameters [14], but did not find any correlation with age in a group of 19 patients. Using the same method on 574 child CT-scans, Daunt et al. found a smaller Haller index for children under two, but a higher index for girls of 0-6 and 12-18 years compared to boys of the same ages [8]. In 1989, Stokes et al. studied the 3D geometry of 71 scoliotic rib cages, compared to 10 controls composed of six cadavers and four volunteers (aged 26 to 54), using stereoradiography reconstruction modeling with 0-20° incidences [28]. Costal cartilage dimensions were estimated from direct measurements on four adult cadavers. Using a similar technique, Delorme et al. studied the effect of surgical correction on the shape of the ribcages of 29 adolescents (mean age 15 ± 1.5 years) by calculating the 3D rotations of the ribs [10]. Costal cartilages were not included in the reconstructions. Bertrand et al. performed more precise 3D rib cage reconstructions on 15 asymptomatic adults (mean age 27 ±8 years), using two simultaneous perpendicular planar X-rays from the EOS system (Biospace Instruments, Paris, France) [3]. While various geometric parameters described the ribs, the costal cartilage and sternum were not investigated, due to the lack of visibility. Due to the superimposition of bone structures and the high quantity of radiotransparent cartilage, it is difficult to have a precise quantitative description of child cartilage using standard X-rays.

Another anatomic part of the thorax is the sternum, which influences the global stiffness of the rib cage, and can be used as an osseous age estimator. In 1967, Riach found a high age correlation with the surface of the sternebrae in23 specimens aged between 26 weeks of pregnancy and six-years-old [23]. Nevertheless, the number and time of appearance of the sternebrae show high variations from one child to another; so it seemed not to be a relevant bone-age indicator [1, 21-24].

To take into account growth of cartilage and bone, it is essential to have a better geometrical description of the child ribcage. Thus, the aim of this study is to quantify the 3D geometry and to study the age effect of the child rib cage: including sternum, ribs and costal cartilage, using reconstructions from CT-Scan data.

2. Methods

2.1. Population

Forty-eight thoracic CT-scans of children aged from four months to 15 years (22 girls, 26 boys) were collected and anonymized in the Necker Hospital (Paris, France). The CT-scans had previously been performed on medical prescriptions with consecutive slices of 4 or 5 mm thickness. The clinical prescriptions for CT-scans of the thorax were: severe asthma, acute respiratory distress syndrome, investigation of intrathoracic lymph nodes, inhaled foreign body, trauma with no bone lesion, staging of primary extrathoracic malignancies. CT-scans in children with syndromes or heart congenital lesions were excluded. CT-scans showing thorax abnormalities or recent surgery were not included. Four groups of 12 children were defined according to age: four months to three years (A group), four to seven years (B group), eight to 11 years (C group) and then 12 to 15 years old (D group).

2.2. 3D reconstruction method

An automatic segmentation and reconstruction of the ribs and ossified sternebrae was performed on each transversal plane using Avizo software (V5, VSG, USA), with further manual corrections at the boundaries of the sternebrae. A manual segmentation of the costal cartilages was accomplished to assess both their shape and the junction to the sternum. This thorough segmentation was performed by a pediatric orthopedic surgeon previously trained in radiological identifications and supervised by a pediatric radiologist. A total of 113 sternal sternebrae, 960 ribs and 518 costal cartilages were reconstructed. The sternal cartilage and some costal cartilage were not considered because incomplete or too difficult to discern on the CT-scan images (Table 1). In order to assess the reliability of the resulting sternebrae volume, 102 sternebrae were reconstructed twice, four weeks apart.

2.3. Data processing and calculated parameters

From the 3D reconstructions, each rib was modeled by its mid-line, according to the following steps (Figure 1):

1. The least square circle of the rib was calculated, defining center O and plane A.
2. From the anterior to the posterior extremities, fifty equidistant-angle planes P_i rotating through O, orthogonal to plane A, were created.
3. Fifty corresponding cross sections S_i were calculated as the intersection of planes P_i and the external 3D surface of the rib.
4. The rib mid-line was constructed as the geometric centroid of all S_i sections.

Applied to all left and right ribs, a wireframe of the thorax was then constructed (Figure 2). A similar method was applied to calculate the costal cartilage mid-line. Unlike ribs, costal cartilages are not curved in the transversal plane, so the intersection planes were then defined as parallel to the sagittal plane.

Rib cage morphometry was described by three parameters: maximum anteroposterior width, maximum lateral width, and thoracic index, their ratio. The local quantitative description of the ribs and the costal cartilage was calculated using rib mid-line length, chord length, enclosed area, maximum width, frontal and lateral orientations of the rib [3, 7, 16, 18]. In order to estimate the relative length of the cartilage, the costal index was defined: for each rib, it describes the ratio between the cartilage mid-line length and the whole costal segment, i.e. rib and cartilage mid-line lengths.

2.4. Statistical analysis

Because no assumption was made regarding the distribution of the data, the Kruskal-Wallis test was used to assess the statistical significance of differences in terms of gender, laterality, age group and rib level; with a threshold *p-value* below 0.05 being used to denote significance.

3. Results

3.1. Reconstruction assessment

The reproducibility study performed on 102 sternal elements showed a mean volume difference of 2.7 % (max 9.9 %, Standard Deviation 2.3 %), i.e. 0.2 cm^3 (max 2.0 cm^3, SD 0.4 cm^3).

3.2. Sternebrae distribution

Most of the sternums presented a manubrium composed of one sternebra and a mesosternum composed of three sternebrae. A high variability of anatomical configurations was found. For example, Figure 3 shows one immature sternum (a. subject 10; 3-years-old), two sternums with merged sternebrae (b. subjects 33 and 18; 10 and 5-years-old respectively), and two early-adult sternums (c. subjects 26 and 28; 8 and 9-years-old respectively). In three cases, the manubrium had two ossification centers in a vertical disposition. The uppermost part of the mesosternum was always composed of a single ossification center. The lowest part of the mesosternum often exhibited lateral or/and longitudinal bifid ossification centers. The xiphoid process was already ossified in seven cases before six years old (out of 18 cases).

While the distribution of the sternebrae was found to be highly variable, Figure 4 shows the evolution of the sternebrae volumes of each sternum during growth. A global increase was observed and an exponential equation was fitted to describe sternum volume versus age relation of the studied population. The volumes were significantly different between all age groups ($p < 10^{-4}$) and the volume of the 15-year-old sternum is about 10 times the volume at birth. Furthermore, dispersion is higher for the oldest patients. No significant difference was found between girls and boys with regard to the sternal volume distribution ($p > 0.8$).

3.2. Ribs and rib cage geometry

Statistical tests did not show significant differences for any parameter, either for gender ($p > 0.15$) or laterality ($p > 0.95$). Consequently, in the first approach, no distinction is made between girls and boys, left and right ribs or costal cartilages.

The global parameters of the rib cages are summed up in Table 1. The lateral (LAT) and anteroposterior (AP) widths increase with age, but the thoracic index shows a very small increase during growth.

In Figure 5, the mean and SD costal index is plotted for each rib level by age group. For all groups, the costal index decreases from rib level 1 to 3 and increases from level 3 to 7. Furthermore, the costal index is higher for the first years of life, with an almost equal length of cartilage and bone for levels 1 and 6 (ratio of 47 % and 45 % respectively) for group A. Level 7 has the longest cartilage region in the youngest group with a ratio of 60 %. For all levels, the mean costal index decreases significantly by 21 % between groups A (0 to 3 years old) and B (4 to 7 years old) ($p < 10^{-4}$).

In Figure 6, the progression of ribcage parameters is plotted by age group and rib level. Rib area, rib mid-length, maximum width and chord length increase with age. Rib angles show a small variation in the present population. All the parameters have a similar pattern of evolution regarding rib level. The statistical significance of differences between adjacent groups (A-B, B-C and C-D) have been calculated (Table 2): the geometric rib parameters are significantly different ($p<10^{-4}$) between two adjacent groups, except for the frontal and lateral angles.

With respect to costal and cartilage parameters, Table 3 (supplementary material) sums up the mean values and standard deviations of all calculated parameters. Except for the frontal and lateral orientations of the rib, the mean values of all costal parameters increase from level 1 to level 6, and then decrease from level 7 to level 10. Cartilage length increases with the rib level, from level 1 to 7.

4. Discussion

This study characterizes the bony and cartilaginous structures of the child thorax during its growth, from CT-scan data. Even if the subjects in this cohort were not fully healthy, the CT-scans were prescribed for a list of indications that do not affect the ribcage geometry. Performing CT-scans in healthy children without clinical indication is not possible due to ethical considerations. In this study, only CT-scans performed for limited pathologies were collected, while patients with chest malformations or chronic diseases with potential consequences for the child's growth were excluded. The dataset is therefore believed to be pertinent to represent non-pathological geometries of the child ribcage. The number of subjects is large (48) and covers a wide range of ages, from four months to 15 years, with three subjects per year. The gender distribution of the study population is well balanced. The reconstructions made using the Avizo software have been validated by an intra-observer reproducibility study on 102 sternebrae. Although the detection of bone pixels was automatic, an operator correction was required when two different bone structures were in contact. It was then necessary to distinguish boundaries manually.

As expected, the results show an increase of all parameters with growth. The originality of this study lies in its quantitative approach. The thoracic index of the present study shows a slight evolution during growth, up to 11 years; it then stabilizes (Table 1). Furthermore, the thoracic index shows no significant evolution between children and adults: Bertrand et al. (2008) evaluated this parameter at a mean value of 0.63 (SD 0.07) on 15 adults (mean age: 27 years, SD 8 years), whereas the present child population shows a mean thoracic index of 0.65 (SD 0.05). The thicknesses of the ribs were not taken into account in the present study; therefore the maximum anteroposterior and lateral widths of the thorax morphometric parameters have been slightly underestimated.

The evolution of all the costal parameters for each rib level are compared to a young asymptomatic adult population [3] (Figure 6). The mean growth speed, observed as the distance between the different curves of the same parameter, is not the same between groups, depending on the parameter considered. The differences between 2 adjacent age groups are significant except for frontal and lateral angles (Table 2). Because various body parts are known to have different growth timing [4, 6], no assumptions were made with respect to the growth shape or the variations between the various parameters, even if global growth was expected. Therefore due to the similar proportions in the ribcage dimensions between children and adults, child geometric data can be built from that of adults using an appropriate scaling factor.

Comparison of frontal and lateral angles with adults is difficult due to differences in methodology: while Bertrand et al. studied biplanar X-rays in standing position, the present study is based on CT-scan data, performed on children in a lying position [3]. This is the main limitation of this study: CT-scans were performed in a lying position, together with the unknown respiratory phase during acquisition. These conditions require a careful interpretation of the angular parameters of ribs in frontal and sagittal planes, as the effect of the posture on the thoracic structures (supine versus upright versus seated) has already been underlined [2, 17]. Similarly, for the youngest children, the presence of clothing or diaper can change the natural angle of the ribs, as well as the anteroposterior diameter of the rib cage, as calculated. However, the other parameters are not affected by the lying position as they are calculated using the rib and cartilage mid-lines. The costal index presented in this study gives the cartilage length for the corresponding rib length, for a specific age and rib level. This result - rarely reported in the literature - is essential in a model design because cartilage is a chest component with different mechanical properties and behavior from ribs that are ossified [13]. The current results allow estimates based on *in vivo* measurements.

The sternum is a structure that gradually ossifies. According to the literature, the number and distribution of sternebrae vary with growth. In 1967, by taking anteroposterior radiographs of specimens excised at necropsy, Riach found a correlation between the sum of the sternebrae surfaces and age, especially for the youngest children, less than six years old [23]. Considering the total volume of the sternebrae (Figure 4), the present study completes this trend for older children, up to age 15. Contrary to the number of sternebrae, the volume of the bony parts of the sternum is found to be a good age-predictive parameter, especially for the youngest. An exponential trend fits with age for the population studied. The consequences of growth will probably decline after puberty. Due to the high sensitivity of the results to the age, any conclusion on a gender effect would be uncertain: the age effect will overwhelm the gender effect.

Results from the present study could help to complete missing data or to validate numerical child models. Indeed, various models from the literature used X-rays to reconstruct the 3D geometry of the bony structures of the child rib cage [12, 16]. The costal cartilage, not visible on standard X-rays, is then often approximated. When geometry is unknown in a child model, it is often scaled from the adult ones [15, 27, 30]. Besides the known ratio variation of the geometry and mass of the body segments with growth [6, 25], children's ribcages contain a substantial quantity of growth cartilage, which has different material properties. The present results provide new quantitative data on child ribcage geometry which will assist in building more relevant child numerical models.

To refine the interpretation of the results, it would have been interesting to distinguish between girls and boys according to their respective puberty growth. However, it then would have been necessary to obtain data on a higher number of patients that had passed the peak of puberty, until 17 or 18 years old. The same protocol could be used in further studies for such assessment.

Finally, the present study highlighted the cartilaginous preponderance and the evolution of the young thorax geometry compared to that of adults. Thus such data could help to improve the biofidelity of child models for the thoracic segment. Future applications could be considered, like the improvement of Finite Element Models [19], physical dummies for CPR training [20], forensic analysis, or to define the standard geometry of the paediatric thorax and help to detect clinical abnormalities.

Acknowledgements

The authors gratefully acknowledge the kind review of C. Adam. This research was partly funded by a grant from the ANR (SECUR_ENFANT 06_0385) and supported by the GDR 2610 “Biomécanique des chocs” (CNRS/INRETS/GIE PSA Renault).

References

1. Ashley G. T. (1956) The relationship between the pattern of ossification and the definitive shape of the mesosternum in man. J Anat 90:87.
2. Beillas P., Lafon Y., Smith F. W. (2009) The effects of posture and subject-to-subject variations on the position, shape and volume of abdominal and thoracic organs. Stapp Car Crash J 53:127-54.
3. Bertrand S., Laporte S., Parent S. et al (2008) Three-dimensional reconstruction of the rib cage from biplanar radiography. IRBM 29(4):278.
4. Beusenberg M. C., Happee R., Twisk D. et al. *Status of injury biomechanics for the development of child dummies*. in *Child Occupant Protection Symposium*. 1993. San Antonio, Texas, USA.
5. Brown J. K., Jing Y., Wang S. et al (2006) Patterns of severe injury in pediatric car crash victims: Crash Injury Research Engineering Network database. J Pediatr Surg 41(2):362-7.
6. Burdi A. R., Huelke D. F., Snyder R. G. et al (1969) Infants and children in the adult world of automobile safety design: pediatric and anatomical considerations for design of child restraints. J Biomech 2(3):267-80.
7. Dansereau Jean, Stokes Ian A. F. (1988) Measurements of the three-dimensional shape of the rib cage. Journal of Biomechanics 21(11):893.
8. Daunt S. W., Cohen J. H., Miller S. F. (2004) Age-related normal ranges for the Haller index in children. Pediatric Radiology 34(4):326.
9. de Jager Kate, van Ratingen Michiel, Lesire Philippe et al. *Assessing new child dummies and criteria for child occupant protection in frontal impact*. in *19th ESV Conference*. 2005. TNO - LAB - BASt - IDIADA - UTAC.
10. Delorme S., Violas P., Dansereau J. et al (2001) Preoperative and early postoperative three-dimensional changes of the rib cage after posterior instrumentation in adolescent idiopathic scoliosis. European spine journal : official publication of the European Spine Society, the European Spinal Deformity Society, and the European Section of the Cervical Spine Research Society 10(2):101-7.
11. Derveaux L., Clarysse I., Ivanoff I. et al (1989) Preoperative and postoperative abnormalities in chest x-ray indices and in lung function in pectus deformities. Chest 95(4):850.
12. Dworzak J., Lamecker H., von Berg J. et al (2010) 3D reconstruction of the human rib cage from 2D projection images using a statistical shape model. International journal of computer assisted radiology and surgery 5(2):111-24.
13. Forman J. L., Kent R. W. (2011) Modeling costal cartilage using local material properties with consideration for gross heterogeneities. J Biomech 44(5):910-6.
14. Haller J. A., S. Kramer S., A. Lietman S. (1987) Use of CT scans in selection of patients for pectus excavatum surgery: a preliminary report. J Pediatr Surg 22(0022-3468).

15. Irwin Annette L., Mertz Harold J. *Biomechanical bases for the CRABI and Hybrid III child dummies*. in *41st Stapp Car Crash Conference*. 1997. Lake Buena Vista, Florida, USA.
16. Jolivet E., Sandoz B., Laporte S. et al (2010) Fast 3D reconstruction of the rib cage from biplanar radiographs. Med Biol Eng Comput 48(8):821-8.
17. Lafon Y., Smith F. W., Beillas P. (2010) Combination of a model-deformation method and a positional MRI to quantify the effects of posture on the anatomical structures of the trunk. J Biomech 43(7):1269-78.
18. Mitton D., Zhao K., Bertrand S. et al (2008) 3D reconstruction of the ribs from lateral and frontal X-rays in comparison to 3D CT-scan reconstruction. J Biomech 41(3):706-10.
19. Mizuno K., Iwata K., Deguchi T. et al (2005) Development of a three-year-old child FE model. Traffic Inj Prev 6(4):361-71.
20. Nishisaki Akira, Nysaether Jon, Sutton Robert et al (2009) Effect of mattress deflection on CPR quality assessment for older children and adolescents. Resuscitation 80(5):540.
21. O'Neal M. L., Dwornik J. J., Ganey T. M. et al (1998) Postnatal development of the human sternum. Journal of Pediatric Orthopaedics 18(3):398.
22. Ogden J. A., Conlogue G. J., Bronson M. L. et al (1979) Radiology of postnatal skeletal development - II. The manubrium and sternum. Skeletal Radiology 4(4):189.
23. Riach I. C. (1967) Ossification in the sternum as a means of assessing skeletal age. Journal of Clinical Pathology 20(4):589.
24. Rush W. J., Donnelly L. F., Brody A. S. et al (2002) "Missing" sternal ossification center: Potential mimicker of disease in young children. Radiology 224(1):120.
25. Sandoz B., Laporte S., Skalli W. et al (2010) Subject-specific body segment parameters' estimation using biplanar X-rays: a feasibility study. Comput Methods Biomech Biomed Engin 13(6):649-54.
26. Saul Roger A., Pritz Howard B., McFadden Joeseph et al. *Description and performance of the Hybrid III three-year-old, six-year-old and small female test dummies in restraint system and out-of-position air bag environments*. in *16th International Technical Conference on the Enhanced Safety of Vehicles*. 1998. NHTSA (National Highway Traffic Safety Administration).
27. Schneider K., Zernicke R. F. (1992) Mass, center of mass, and moment of inertia estimates for infant limb segments. J Biomech 25(2):145-8.
28. Stokes I. A., Dansereau J., Moreland M. S. (1989) Rib cage asymmetry in idiopathic scoliosis. Journal of orthopaedic research : official publication of the Orthopaedic Research Society 7(4):599-606.
29. van Ratingen Michiel R., Twisk Dirk, Schrooten Mark et al. *Biomechanically based design and performance targets for a 3-year-old-child crash dummy for front and side impact*. in *Second Child Occupant Protection Symposium*. 1997. Lake Buena Vista, Florida, USA.
30. Wang Y., Rangarajan N., Shams T. et al (2005) *Design of a biofidelic instrumented 3.4 kg infant dummy*, NHTSA (National Highway Traffic Safety Administration).

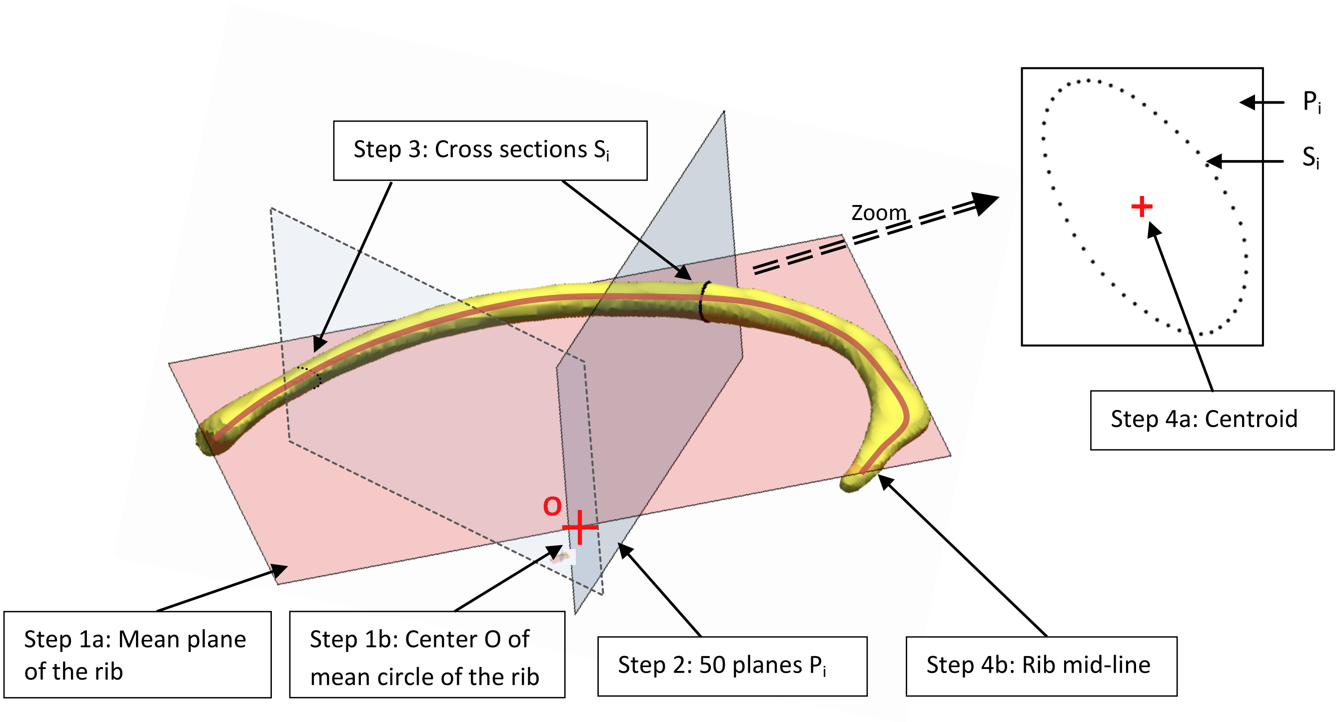

Figure 1: Rib mid-line calculation steps.

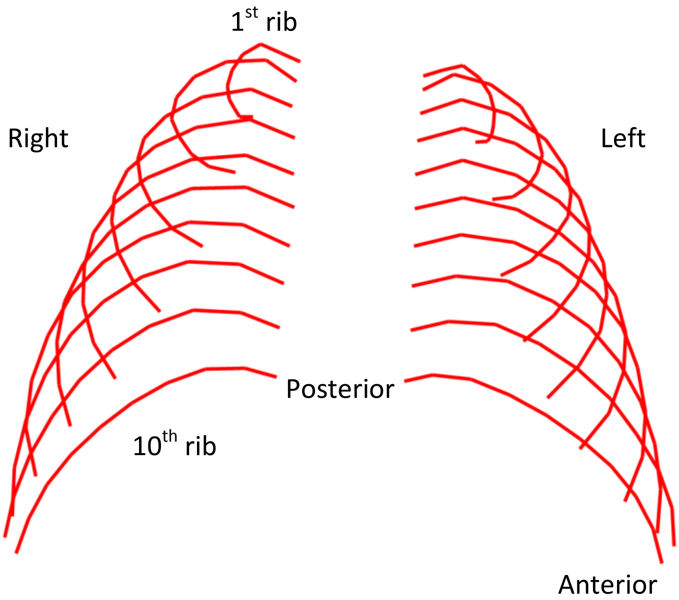

Figure 2: Calculated mid-lines rib cage (patient 10).

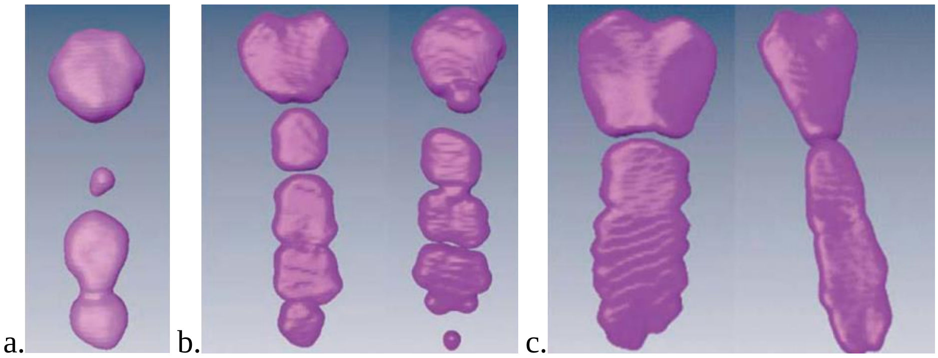

Figure 3: Various sternum configurations, high variability not correlated to age.
a. immature sternum (3 years old); b. merged sternebrae (10 and 5 yo); c. early-adult sternums (8 and 9 yo).

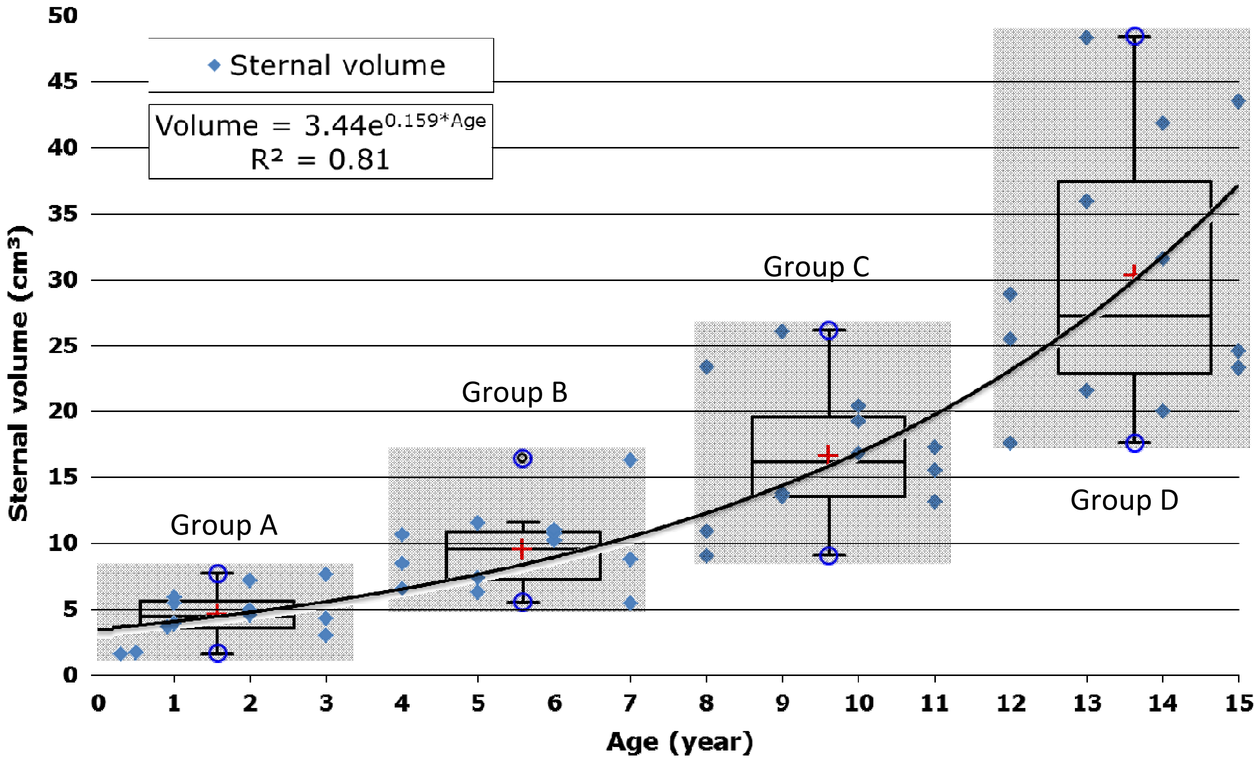

Figure 4: Measured sternebrae volume evolution with age, and boxplots by age groups. Group A: 0.3 to 3 years old; Group B: 4-7 yo; Group C: 8-11 yo; Group D: 12-15 yo. The volumes are significantly different between all age groups ($p < 10^{-4}$).

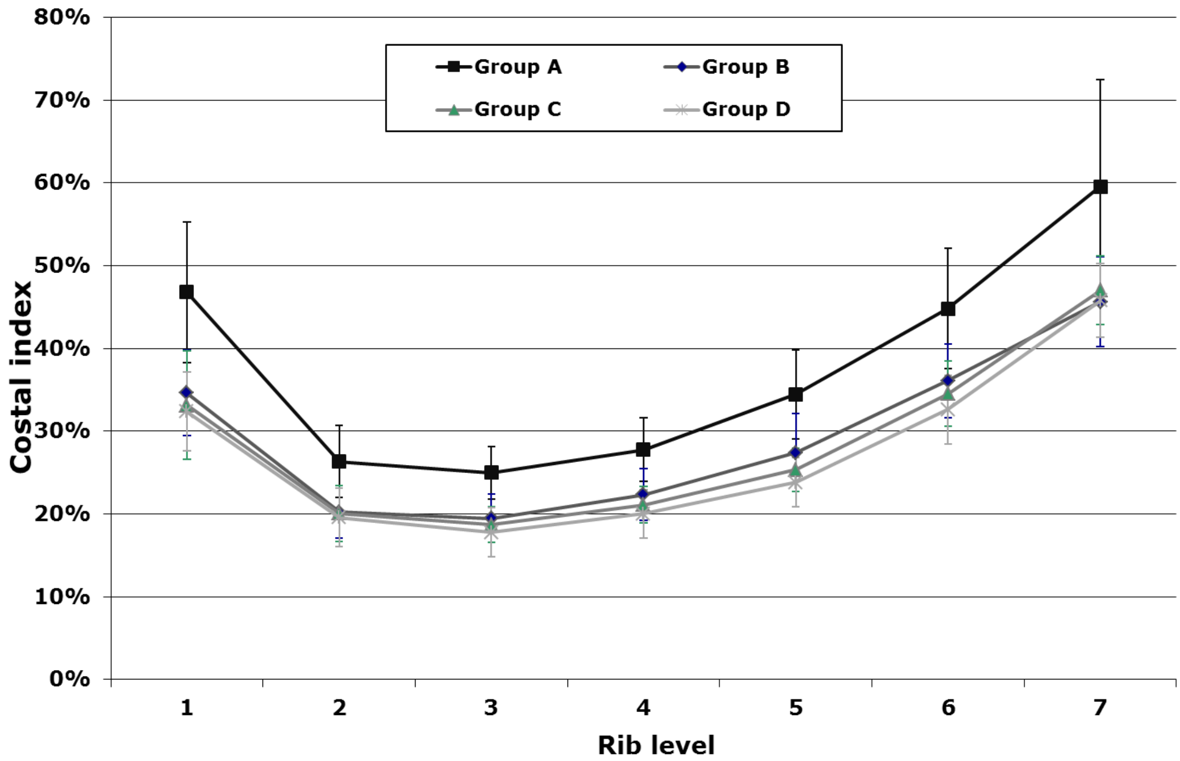

Figure 5: Costal index (mean and standard deviation) function of rib level and age group. Group A: 0.3 to 3 years old; Group B: 4-7 yo; Group C: 8-11 yo; Group D: 12-15 yo.

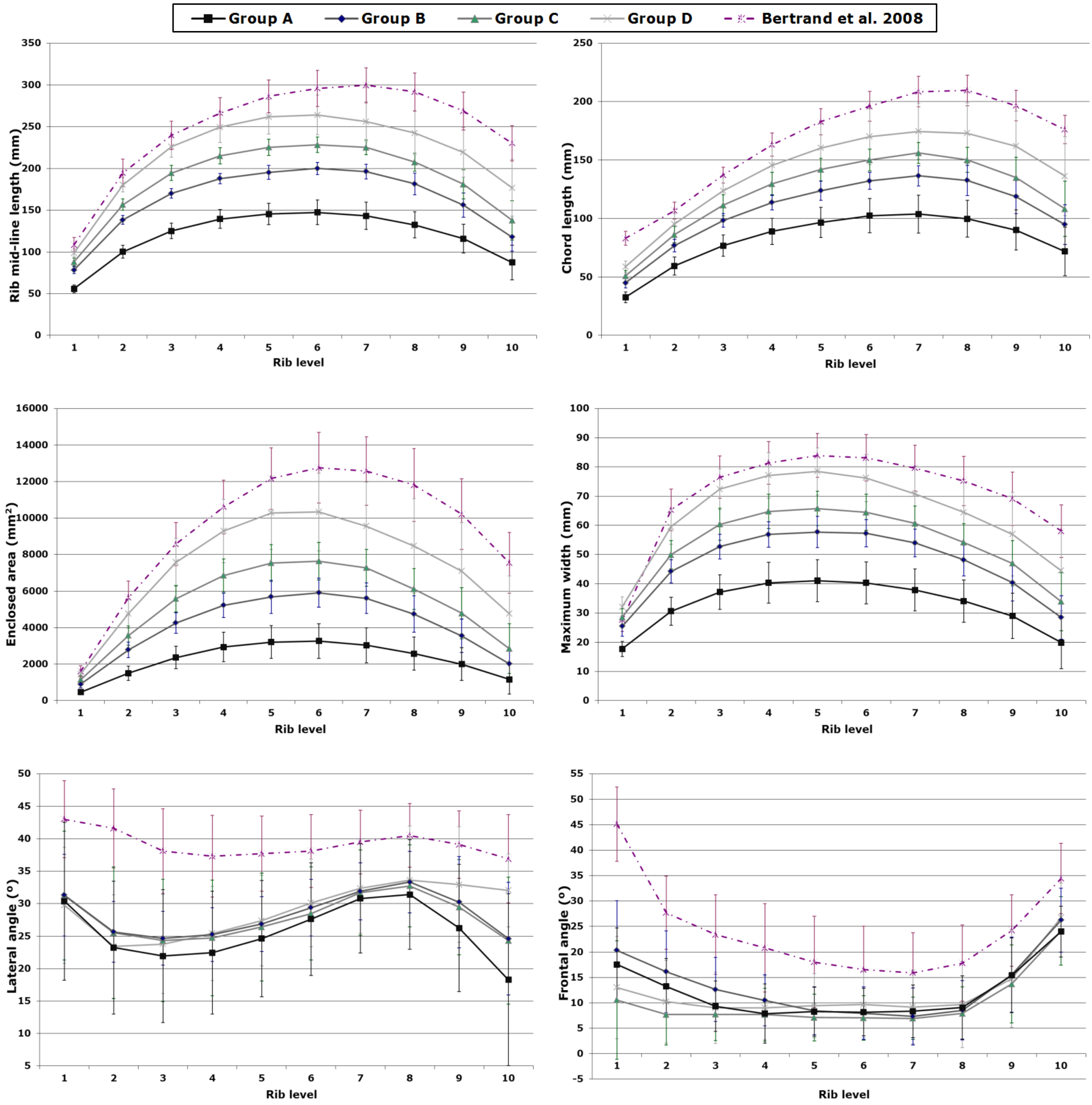

Figure 6: Evolution of parameters and comparison with the literature, function of rib level and age group (mean and standard deviation). Group A: 0.3 to 3 years old; Group B: 4-7 yo; Group C: 8-11 yo; Group D: 12-15 yo; Bertrand et al. (2008): 27 yo (SD 8 yo).

Supplementary material - Table 3: Mean (SD) rib and cartilage calculated parameters, 3 children per age group.

		Age (year)															
Data	**Rib level**	**< 1**	**1**	**2**	**3**	**4**	**5**	**6**	**7**	**8**	**9**	**10**	**11**	**12**	**13**	**14**	**15**
Rib length (mm)	1	45.0 (5.6)	57.5 (2.9)	58.1 (3.1)	62.9 (1.6)	79.4 (14.1)	76.1 (5.9)	76.1 (3.6)	81.7 (8.5)	86.3 (8.9)	85.5 (7.4)	85.6 (8.8)	94.9 (3.5)	89.6 (9.1)	103.0 (4.7)	100.8 (7.4)	100.8 (7.5)
	2	80.7 (9.4)	100.3 (9.7)	107.3 (5.4)	112.5 (5.3)	131.8 (13.3)	140.4 (8.9)	134.1 (5.1)	146.7 (11.6)	151.4 (12.2)	146.1 (8.9)	159.0 (6.1)	170.1 (3.7)	166.1 (15.0)	189.4 (10.4)	183.9 (9.0)	182.3 (21.1)
	3	99.9 (10.4)	124.9 (10.3)	135.4 (4.7)	140.4 (5.7)	161.6 (13.1)	170.8 (9.6)	166.4 (4.3)	181.6 (10.2)	186.8 (13.9)	184.0 (9.8)	200.2 (3.9)	207.1 (2.1)	206.8 (13.7)	234.2 (18.0)	234.4 (10.7)	228.5 (26.9)
	4	109.1 (11.5)	138.3 (10.9)	152.5 (4.8)	157.3 (6.9)	178.6 (13.2)	188.0 (10.2)	183.4 (4.0)	201.2 (8.7)	205.6 (15.6)	204.1 (11.9)	224.3 (4.5)	225.9 (2.8)	226.5 (16.8)	258.2 (24.1)	262.6 (10.4)	250.5 (29.3)
	5	113.0 (12.1)	144.3 (8.8)	161.4 (4.6)	162.7 (9.0)	186.0 (12.9)	196.6 (10.9)	186.3 (17.4)	212.1 (9.2)	215.3 (17.9)	217.4 (15.4)	235.1 (5.4)	233.5 (4.7)	236.7 (16.4)	275.4 (25.6)	273.8 (10.8)	261.4 (31.2)
	6	112.7 (12.3)	146.2 (6.8)	163.5 (6.0)	166.9 (8.3)	189.2 (13.5)	201.4 (10.5)	195.7 (3.8)	213.9 (10.9)	219.4 (18.3)	220.5 (15.0)	238.5 (3.0)	234.9 (7.5)	239.2 (15.1)	277.4 (31.3)	275.9 (9.5)	263.4 (34.7)
	7	110.2 (12.7)	135.4 (9.4)	160.5 (6.4)	166.7 (7.7)	185.6 (13.3)	194.9 (16.1)	193.1 (3.7)	211.1 (11.2)	215.3 (18.0)	217.9 (15.2)	234.5 (1.8)	233.0 (5.9)	234.1 (13.8)	257.2 (49.5)	270.5 (9.4)	262.3 (35.9)
	8	104.4 (12.4)	122.3 (16.0)	146.9 (10.8)	155.9 (12.3)	177.1 (13.2)	178.2 (25.8)	176.9 (12.9)	193.4 (23.2)	188.2 (12.1)	203.8 (16.1)	225.8 (1.1)	211.9 (16.1)	223.0 (12.0)	233.7 (68.1)	259.0 (9.4)	253.4 (34.5)
	9	95.1 (11.3)	100.9 (20.3)	128.4 (22.3)	139.0 (18.8)	157.6 (7.3)	154.1 (31.8)	155.5 (19.5)	156.9 (25.7)	152.4 (8.4)	180.9 (20.4)	207.6 (5.6)	183.0 (32.6)	202.7 (10.7)	203.7 (85.8)	237.5 (8.2)	233.1 (27.9)
	10	80.9 (8.4)	60.7 (16.9)	97.4 (34.4)	110.6 (25.9)	124.4 (8.8)	115.2 (32.2)	122.8 (20.5)	109.0 (30.8)	103.3 (7.4)	139.0 (20.7)	174.3 (6.7)	140.2 (41.5)	162.6 (9.6)	148.9 (85.8)	199.5 (7.6)	195.6 (19.7)
Cartilage length (mm)	1	22.8 (2.9)	27.2 (0.1)	25.6 (3.6)	27.3 (2.8)	27.0 (0.8)	29.5 (3.0)	24.0 (3.4)	26.6 (1.3)	32.8 (4.2)	29.8 (6.3)	27.2 (5.2)	22.4 (4.1)	28.9 (4.0)	32.7 (3.4)	33.0 (5.5)	32.6 (4.9)
	2	23.7 (3.8)	28.1 (1.0)	27.1 (2.9)	26.8 (2.9)	28.6 (2.5)	26.9 (3.5)	25.9 (5.5)	29.6 (3.6)	32.7 (1.1)	30.8 (6.2)	30.4 (4.1)	28.5 (0.6)	30.9 (4.1)	34.2 (5.0)	37.8 (6.0)	37.4 (5.0)
	3	28.1 (3.6)	34.3 (1.3)	32.1 (2.0)	30.9 (3.2)	35.3 (1.9)	32.2 (5.4)	32.0 (7.2)	33.6 (1.5)	37.6 (2.2)	35.5 (6.2)	35.4 (2.9)	34.4 (1.0)	35.3 (2.6)	39.0 (5.8)	42.4 (6.8)	42.8 (5.9)
	4	34.2 (4.3)	43.3 (1.3)	39.1 (3.4)	38.1 (4.5)	44.5 (1.7)	40.9 (7.0)	42.1 (7.1)	41.7 (2.6)	47.4 (3.2)	44.5 (5.2)	42.8 (3.2)	45.4 (1.4)	45.7 (4.7)	47.8 (5.8)	52.6 (6.7)	52.6 (8.1)
	5	42.5 (4.0)	56.4 (4.4)	48.9 (2.9)	53.7 (10.3)	56.0 (1.9)	52.4 (8.0)	53.9 (8.7)	52.1 (5.0)	59.5 (4.6)	55.4 (4.3)	54.1 (4.6)	57.7 (3.4)	55.6 (2.8)	61.2 (8.3)	65.7 (8.4)	66.0 (9.0)
	6	60.2 (5.5)	73.9 (6.9)	65.6 (2.6)	63.7 (0.7)	76.2 (1.8)	71.5 (11.8)	64.2 (2.1)	74.9 (5.9)	83.2 (3.2)	74.2 (5.5)	75.6 (7.9)	82.7 (4.2)	80.0 (4.4)	78.2 (6.6)	90.7 (9.5)	94.0 (11.0)
	7	70.7 (1.2)		87.1 (2.4)	79.4		98.3 (24.0)	83.6 (4.4)	100.7 (9.3)		105.2 (9.0)	105.7 (10.3)		114.0 (9.0)	110.6 (9.2)	128.7 (7.2)	125.1 (11.1)
Chord length (mm)	1	26.0 (3.1)	34.3 (1.0)	33.8 (2.2)	36.5 (2.2)	44.3 (6.8)	43.9 (2.2)	45.6 (4.7)	45.9 (2.3)	49.8 (5.0)	49.8 (5.0)	48.9 (3.8)	55.1 (1.4)	55.4 (4.4)	62.3 (4.1)	59.9 (4.6)	57.3 (3.9)
	2	47.8 (4.6)	61.3 (2.7)	63.7 (4.8)	64.5 (2.4)	73.1 (5.7)	77.3 (5.1)	77.7 (5.0)	79.1 (4.2)	83.0 (5.0)	82.9 (7.7)	84.5 (3.0)	94.3 (4.9)	92.6 (6.1)	97.9 (5.4)	98.6 (8.7)	92.3 (12.8)
	3	62.9 (3.8)	79.4 (4.8)	82.3 (5.9)	82.6 (2.2)	92.8 (6.6)	99.6 (5.8)	99.6 (4.5)	101.4 (1.8)	108.3 (5.7)	108.5 (12.5)	107.6 (2.5)	120.8 (5.8)	116.6 (5.7)	127.7 (7.6)	131.1 (10.0)	119.2 (19.3)
	4	71.8 (4.3)	92.3 (4.9)	95.3 (6.7)	96.4 (3.6)	107.2 (7.1)	116.0 (6.5)	114.3 (3.4)	117.5 (2.4)	125.8 (7.2)	125.5 (12.9)	127.7 (5.7)	139.2 (6.2)	134.9 (6.9)	152.5 (12.4)	157.1 (14.5)	137.9 (26.5)
	5	77.2 (5.4)	99.4 (5.8)	104.7 (6.9)	105.3 (3.4)	116.6 (7.5)	128.0 (6.6)	121.5 (9.2)	128.9 (2.1)	137.5 (6.8)	136.8 (11.1)	142.4 (7.9)	151.2 (5.7)	147.6 (8.5)	169.5 (13.4)	171.8 (15.3)	152.3 (31.0)
	6	80.7 (6.0)	103.5 (7.1)	111.1 (8.0)	114.4 (2.1)	124.0 (8.0)	135.6 (6.9)	131.8 (1.6)	137.1 (2.6)	146.2 (7.3)	144.8 (11.1)	150.8 (8.0)	158.4 (5.0)	156.0 (8.8)	180.2 (16.8)	182.6 (16.9)	161.3 (36.3)
	7	81.9 (6.7)	99.1 (6.8)	113.8 (7.0)	120.6 (3.6)	128.2 (8.2)	138.8 (11.0)	135.5 (2.1)	143.4 (2.9)	151.5 (7.3)	151.1 (9.6)	157.5 (7.7)	163.9 (5.0)	163.9 (11.3)	176.0 (21.5)	188.8 (15.9)	169.6 (36.5)
	8	80.3 (6.5)	94.4 (10.7)	107.8 (5.6)	116.5 (7.6)	128.5 (10.0)	132.4 (18.6)	129.7 (6.8)	139.7 (13.6)	138.2 (5.3)	148.8 (11.5)	159.2 (4.8)	154.3 (7.1)	163.6 (9.9)	168.2 (37.4)	188.2 (13.3)	171.7 (31.9)
	9	75.3 (6.4)	80.6 (12.9)	97.4 (14.2)	107.2 (12.7)	118.3 (7.4)	119.0 (22.2)	118.3 (11.2)	119.4 (16.8)	116.5 (5.5)	135.0 (15.6)	151.4 (2.2)	136.9 (19.9)	155.0 (7.7)	150.3 (51.1)	179.5 (10.7)	163.1 (26.9)
	10	66.4 (5.0)	53.2 (13.0)	78.3 (23.7)	89.3 (18.4)	98.4 (6.5)	94.1 (23.3)	97.8 (13.2)	88.8 (21.9)	84.7 (5.7)	109.8 (16.5)	132.5 (3.1)	109.8 (28.5)	129.6 (6.6)	115.6 (59.6)	156.8 (9.6)	142.9 (21.7)
Enclosed area (mm^2)	1	296 (77)	489 (53)	508 (49)	585 (34)	935 (344)	838 (117)	854 (87)	980 (190)	1100 (238)	1077 (180)	1089 (209)	1356 (88)	1213 (248)	1589 (166)	1535 (230)	1504 (203)
	2	969 (231)	1508 (274)	1705 (148)	1838 (188)	2532 (476)	2854 (385)	2630 (231)	3108 (433)	3314 (518)	3099 (331)	3655 (253)	4196 (169)	4068 (714)	5183 (473)	4948 (497)	4878 (1024)
	3	1491 (322)	2332 (355)	2725 (165)	2915 (260)	3834 (562)	4323 (495)	4069 (203)	4811 (483)	5138 (736)	4952 (472)	5899 (304)	6360 (124)	6385 (866)	8118 (1095)	8036 (699)	7789 (1746)
	4	1791 (403)	2843 (419)	3471 (197)	3653 (342)	4728 (649)	5266 (576)	4944 (165)	5945 (464)	6223 (899)	6104 (678)	7459 (399)	7617 (230)	7672 (1146)	10033 (1738)	10061 (706)	9406 (2089)
	5	1929 (433)	3091 (341)	3885 (189)	3928 (449)	5175 (712)	5781 (676)	5152 (862)	6640 (545)	6818 (1114)	6926 (962)	8269 (409)	8130 (365)	8370 (1218)	11385 (1986)	11053 (934)	10335 (2340)
	6	1897 (428)	3150 (222)	3958 (212)	4053 (456)	5325 (772)	6039 (694)	5573 (202)	6716 (687)	6964 (1190)	7033 (1014)	8464 (167)	8095 (558)	8433 (1124)	11467 (2504)	11052 (827)	10395 (2464)
	7	1779 (424)	2681 (393)	3758 (203)	3922 (439)	5087 (761)	5558 (886)	5334 (138)	6455 (766)	6536 (1196)	6726 (1045)	7984 (186)	7852 (327)	7851 (985)	9899 (3857)	10363 (863)	10119 (2307)
	8	1572 (422)	2163 (552)	3138 (480)	3423 (608)	4570 (702)	4583 (1200)	4400 (550)	5412 (1245)	4975 (759)	5800 (922)	7247 (207)	6412 (971)	6973 (740)	8281 (4529)	9279 (889)	9354 (2119)
	9	1292 (362)	1493 (614)	2459 (818)	2761 (779)	3626 (300)	3513 (1339)	3437 (809)	3630 (1126)	3306 (426)	4699 (977)	6203 (437)	4934 (1632)	5778 (640)	6788 (4974)	7797 (716)	8043 (1614)
	10	902 (233)	469 (278)	1482 (962)	1777 (829)	2221 (342)	1958 (1080)	2146 (721)	1751 (912)	1449 (207)	2762 (796)	4394 (371)	3021 (1536)	3669 (445)	4050 (3792)	5590 (426)	5725 (976)
Max width (mm)	1	14.3 (2.2)	18.1 (2.0)	18.3 (0.9)	20.1 (0.8)	26.3 (5.0)	24.1 (1.9)	24.1 (0.8)	27.3 (4.1)	28.5 (3.6)	27.1 (1.9)	28.0 (3.4)	30.6 (2.2)	28.6 (3.8)	33.2 (1.7)	32.3 (2.6)	34.2 (2.7)
	2	24.5 (3.1)	30.3 (3.9)	32.8 (0.8)	35.0 (2.4)	42.6 (4.8)	45.6 (2.9)	41.7 (1.2)	47.2 (4.1)	49.0 (4.7)	44.8 (4.1)	51.6 (1.8)	54.4 (2.5)	53.2 (5.6)	63.6 (4.5)	59.7 (2.5)	61.8 (6.1)
	3	28.9 (3.7)	36.4 (3.1)	40.8 (0.6)	42.7 (2.2)	50.3 (4.8)	53.7 (3.6)	50.0 (0.5)	56.9 (3.1)	57.6 (5.2)	55.6 (5.5)	64.3 (1.9)	64.0 (1.9)	65.5 (5.9)	76.2 (6.7)	72.9 (2.8)	74.9 (7.4)
	4	30.6 (4.1)	38.9 (3.1)	45.3 (0.6)	46.6 (2.4)	54.6 (4.5)	57.2 (3.9)	54.1 (0.9)	61.6 (3.2)	61.2 (5.5)	60.2 (6.2)	70.0 (0.9)	67.7 (2.0)	69.2 (6.7)	80.7 (8.6)	78.7 (2.7)	79.8 (7.0)
	5	31.0 (4.3)	39.9 (2.2)	46.8 (1.2)	46.6 (3.6)	55.6 (4.6)	57.8 (4.2)	54.0 (4.5)	63.4 (3.6)	61.8 (6.4)	62.7 (6.7)	71.0 (0.9)	67.5 (2.5)	70.2 (5.9)	83.1 (9.2)	79.9 (3.9)	80.6 (6.7)
	6	29.9 (4.4)	39.7 (1.4)	45.9 (1.1)	45.8 (3.3)	54.9 (4.5)	57.5 (3.8)	54.5 (1.7)	62.1 (4.4)	60.6 (6.7)	61.6 (6.9)	70.1 (1.2)	65.5 (3.9)	68.8 (5.2)	80.1 (10.9)	77.4 (4.1)	78.5 (6.6)
	7	28.2 (4.4)	36.1 (3.5)	43.7 (1.4)	43.5 (3.2)	52.1 (4.5)	53.1 (4.5)	52.0 (1.1)	58.8 (4.8)	56.5 (6.5)	58.1 (6.5)	65.6 (2.5)	62.5 (3.1)	63.6 (4.1)	71.3 (16.4)	72.7 (4.3)	75.3 (5.5)
	8	26.0 (4.6)	31.1 (4.9)	39.4 (3.7)	39.8 (4.4)	47.8 (3.5)	46.7 (6.5)	46.3 (3.7)	52.0 (6.8)	48.7 (4.5)	52.0 (5.4)	60.8 (2.3)	55.3 (6.2)	58.4 (3.4)	62.0 (20.7)	67.0 (4.1)	70.4 (5.4)
	9	22.8 (4.2)	24.6 (6.3)	33.7 (6.8)	34.9 (5.9)	41.8 (1.6)	39.1 (8.7)	39.8 (6.1)	40.7 (7.7)	39.3 (2.9)	46.3 (4.6)	54.7 (3.4)	47.7 (9.7)	51.3 (3.5)	51.9 (27.3)	60.0 (3.7)	64.6 (3.8)
	10	18.3 (3.0)	11.5 (5.2)	23.3 (10.9)	26.5 (7.8)	31.3 (3.2)	27.0 (9.3)	29.9 (6.3)	25.7 (9.7)	24.2 (1.9)	33.9 (5.1)	44.7 (3.2)	34.4 (12.6)	39.1 (2.5)	36.8 (25.3)	48.9 (2.6)	53.2 (2.3)
Lateral rib angle (°)	1	19.6 (3.1)	23.5 (10.9)	32.3 (4.9)	46.0 (6.1)	33.4 (1.6)	27.2 (8.2)	33.2 (6.5)	31.3 (6.4)	32.4 (4.9)	40.5 (7.3)	26.2 (11.4)	25.9 (8.7)	30.0 (6.6)	28.9 (4.6)	28.4 (14.3)	31.6 (9.5)
	2	14.3 (5.2)	19.7 (10.5)	23.1 (4.0)	35.8 (5.4)	27.8 (1.4)	22.7 (4.6)	27.6 (4.6)	24.4 (5.8)	29.2 (6.5)	34.7 (7.7)	18.3 (10.1)	19.8 (7.1)	24.8 (5.1)	23.4 (5.2)	21.2 (12.2)	24.2 (9.0)
	3	13.5 (6.4)	19.4 (10.7)	21.3 (4.9)	33.5 (7.0)	25.1 (1.7)	23.3 (4.0)	27.3 (4.4)	22.9 (5.1)	28.6 (7.8)	32.3 (8.8)	16.9 (5.7)	19.5 (6.6)	24.9 (3.8)	24.7 (6.0)	21.9 (10.5)	23.7 (9.9)
	4	15.1 (6.3)	21.1 (9.5)	21.2 (4.9)	32.4 (8.5)	24.5 (2.3)	24.1 (4.2)	28.7 (3.7)	23.6 (4.6)	29.2 (7.1)	31.8 (9.6)	17.7 (3.4)	20.2 (6.4)	26.5 (4.3)	27.8 (6.0)	23.1 (9.1)	24.3 (9.5)
	5	19.2 (6.2)	23.9 (8.6)	22.5 (4.4)	32.8 (10.7)	25.4 (2.2)	25.6 (4.3)	30.9 (3.7)	25.5 (4.3)	30.9 (6.7)	32.8 (8.8)	19.9 (2.5)	22.0 (6.5)	29.0 (5.1)	29.8 (5.2)	25.6 (7.9)	25.1 (9.4)
	6	24.5 (6.0)	26.4 (8.1)	24.4 (3.1)	35.1 (11.9)	27.6 (2.5)	27.9 (4.6)	34.5 (2.3)	27.5 (3.7)	33.0 (6.2)	33.7 (7.3)	22.1 (2.1)	25.2 (4.7)	32.0 (6.2)	31.3 (4.8)	29.6 (7.5)	27.5 (8.8)
	7	31.6 (7.3)	27.9 (6.9)	26.6 (2.3)	37.1 (11.7)	29.9 (2.8)	30.3 (4.3)	37.4 (2.5)	30.1 (2.9)	35.8 (6.2)	36.5 (5.7)	24.9 (2.7)	29.6 (3.4)	34.7 (7.2)	31.2 (5.8)	33.6 (6.5)	30.1 (8.8)
	8	34.0 (9.3)	27.6 (5.5)	26.6 (3.7)	37.5 (10.0)	32.7 (4.1)	31.1 (2.3)	38.7 (2.8)	30.8 (5.0)	34.2 (6.9)	38.3 (5.7)	27.2 (3.3)	31.2 (3.6)	35.9 (8.8)	30.1 (10.3)	36.1 (5.7)	32.5 (8.7)
	9	30.3 (9.2)	19.3 (8.6)	22.3 (7.4)	33.0 (8.8)	32.0 (2.8)	27.6 (3.9)	36.8 (3.2)	24.5 (9.4)	27.8 (8.6)	34.3 (7.1)	26.7 (4.4)	29.0 (7.8)	35.4 (9.0)	28.4 (11.6)	36.6 (4.9)	31.3 (8.6)
	10	25.8 (6.4)	8.9 (16.2)	12.8 (12.2)	25.7 (8.9)	27.5 (3.1)	19.4 (9.5)	33.0 (3.9)	18.5 (7.9)	22.0 (12.4)	26.8 (8.4)	21.0 (12.0)	26.5 (7.6)	34.4 (6.6)	30.1 (5.0)	33.1 (5.9)	30.6 (5.2)
Frontal rib angle (°)	1	12.4 (7.6)	14.0 (5.2)	23.1 (4.9)	20.6 (5.8)	19.2 (6.1)	28.6 (8.0)	20.5 (11.4)	13.0 (7.8)	6.4 (4.4)	16.2 (18.9)	15.2 (10.4)	4.4 (3.6)	8.2 (3.7)	12.2 (6.8)	17.0 (13.6)	14.6 (13.0)
	2	9.5 (6.5)	11.3 (4.9)	15.9 (2.9)	16.2 (4.7)	16.5 (6.1)	21.9 (4.2)	15.3 (9.3)	10.8 (8.9)	4.6 (2.6)	9.0 (9.1)	12.2 (4.7)	5.0 (2.6)	5.1 (3.7)	10.1 (5.5)	13.0 (8.4)	12.7 (12.0)
	3	6.3 (4.5)	9.7 (4.0)	10.8 (7.0)	10.5 (3.5)	11.3 (5.1)	18.2 (4.1)	11.1 (7.0)	9.9 (6.2)	5.6 (4.2)	9.0 (7.7)	11.7 (1.9)	4.6 (2.2)	5.5 (3.9)	7.0 (5.9)	11.9 (6.8)	11.5 (9.6)
	4	4.6 (3.9)	9.1 (5.0)	9.2 (7.9)	8.6 (5.8)	9.5 (4.9)	14.6 (5.5)	9.1 (4.1)	8.8 (4.3)	5.0 (4.4)	9.6 (6.6)	11.8 (1.9)	4.4 (3.1)	6.8 (3.9)	6.2 (5.7)	12.5 (6.8)	10.6 (7.2)
	5	5.4 (3.7)	10.2 (4.8)	9.4 (7.0)	8.1 (2.5)	8.9 (4.7)	11.7 (6.0)	6.1 (2.9)	7.0 (3.4)	4.5 (4.4)	8.0 (5.8)	10.7 (2.5)	5.2 (3.2)	8.0 (5.2)	8.4 (5.9)	12.9 (7.6)	8.4 (6.6)
	6	7.1 (4.0)	10.9 (3.5)	9.2 (4.4)	5.5 (5.6)	8.0 (5.2)	10.7 (7.0)	7.5 (4.7)	5.7 (3.0)	5.2 (3.6)	6.8 (5.0)	9.8 (3.6)	6.3 (4.7)	9.0 (6.2)	9.3 (7.5)	13.4 (7.1)	6.8 (4.9)
	7	9.4 (4.7)	11.6 (4.3)	8.1 (2.7)	4.2 (6.3)	7.6 (6.1)	10.6 (6.7)	7.9 (5.3)	3.3 (1.6)	6.9 (2.6)	5.2 (3.7)	8.3 (5.2)	7.4 (5.2)	9.0 (6.8)	9.7 (9.9)	12.7 (6.0)	5.3 (5.2)
	8	5.6 (4.3)	15.8 (6.1)	11.2 (3.1)	3.7 (2.0)	8.4 (6.7)	11.5 (6.8)	7.6 (6.2)	6.5 (3.0)	9.4 (6.2)	7.7 (5.0)	8.0 (5.8)	6.6 (4.7)	10.6 (6.4)	11.9 (13.6)	10.8 (7.8)	5.4 (3.7)
	9	7.7 (3.8)	23.4 (6.3)	17.9 (4.0)	12.6 (4.1)	14.5 (7.5)	17.9 (9.4)	13.0 (8.6)	16.8 (3.7)	17.4 (8.0)	15.6 (5.9)	11.2 (8.0)	10.7 (8.1)	12.0 (10.5)	21.0 (11.5)	16.0 (7.3)	9.8 (5.8)
	10	18.8 (4.2)	28.8 (2.7)	25.2 (2.8)	23.2 (4.3)	24.5 (6.3)	27.8 (8.6)	26.4 (7.6)	26.3 (2.2)	26.0 (6.2)	28.1 (3.8)	21.3 (7.2)	21.1 (7.6)	25.0 (6.8)	31.9 (7.9)	27.3 (6.3)	22.9 (3.0)